Available online at www.sciencedirect.com

ScienceDirect

journal homepage: www.elsevier.com/locate/he

The effect of EGR and hydrogen addition to natural gas on performance and exhaust emissions in a diesel engine by AVL fire multi-domain simulation, GPR model, and multi-objective genetic algorithm

Javad Zareei [a,*], *Abbas Rohani* [a,**], *José Ricardo Nuñez Alvarez* [b]

[a] *Department of Biosystems Engineering, Faculty of Agriculture, Ferdowsi University of Mashhad, Mashhad, Iran*
[b] *Department of Energy, University of the Coast (CUC), Barranquilla, Colombia*

HIGHLIGHTS

- Effect of adding hydrogen to natural gas fuel and EGR ratio on a diesel engine.
- The Gaussian process regression (GPR) was utilized as a tool for modeling engine performance and exhaust emissions.
- Effect of EGR and blend of HCNG on engine performance and exhaust emissions.
- Using a multi-objective genetic algorithm (MOGA).
- The results of GPR and MOGA illustrated that the optimum values of EGR and HCNG were 6.35% and 31%, respectively.

GRAPHICAL ABSTRACT

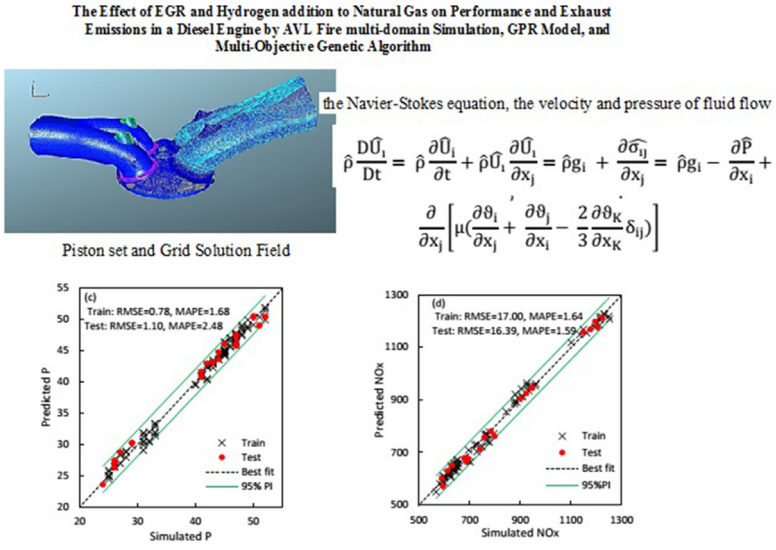

ARTICLE INFO

Article history:
Received 30 January 2022
Received in revised form
2 April 2022
Accepted 29 April 2022
Available online 1 June 2022

ABSTRACT

In this study, the effect of adding hydrogen to natural gas and EGR ratio was conducted on a diesel engine to investigate the engine performance and exhaust gases by AVL Fire multi-domain simulation software.

For this investigation, a mixture of hydrogen fuel and natural gas replaced diesel fuel. The percentage of hydrogen in blend fuel changed from 0% to 40%. The compression ratio converted from 17:1 to 15:1. The EGR ratios were in three steps of 5%, 10%, and 15%, with different engine speeds from 1000 to 1800 RPM. The Gaussian process regression (GPR) was

* *Corresponding author.*
** *Corresponding author.*
E-mail addresses: javadzareei@um.ac.ir (J. Zareei), arohani@um.ac.ir (A. Rohani).
https://doi.org/10.1016/j.ijhydene.2022.04.294

Keywords:
Exhaust gas recirculation
Diesel engine
Performance
Exhaust emissions
Multi-objective genetic algorithm (MOGA)
Cumulative heat release

developed to model engine performance and exhaust emissions. The optimal values of EGR and the percentage of hydrogen in the blend of HCNG were extracted using a multi-objective genetic algorithm (MOGA).

The results showed that by increasing EGR, thermal efficiency, the engine power, and specific fuel consumption decreased due to prolongation of combustion length while cumulative heat release increased but, its effect on cylinder pressure is insignificant. Adding hydrogen to natural gas increased the combustion temperature and, consequently NOx. While the amount of CO and HC decreased. The results of GPR and MOGA illustrated that at different engine speeds, the optimum values of EGR and HCNG were 6.35% and 31%, respectively.

Nomenclatures

EGR	Exhaust gas recirculation
HCNG	Hydrogen + compressed natural gas
FC	Fuel consumption
TE	Thermal efficiency
ANN	Artificial neural network
$\widehat{U}_i$	Local velocity of fluid
$\widehat{\rho}$	Fluid flow density
g_i	gravitational acceleration
$\widehat{P}$	Fluid flow pressure
μ	Cinematic viscosity
ϑ_i , ϑ_j	Stress tensor between fluid flow lines
δ_{ij}	Fluid flow stress with field wall
GPR	Gaussian process regression
KF	Kernel function
QNAH	quasi-Newton approximation to the Hessian
x_{max} and x_{min}	the maximum and minimum values of the input vector (x)
MAPE	The Mean Absolute Percentage Error
RMSE	Root Mean Squared Error

Introduction

One of the most efficient engines available is diesel engines. Due to being economical and for reasons such as moving goods, generating electricity, and carrying passengers, diesel engines are essential. On the other hand, they are one of the sources of environmental pollution and the spread of cancer. Therefore, research in the field of diesel engines is always of interest to researchers [1,2].

The investigation on diesel engines showed that modifying engine geometry, exhaust gases recirculation (EGR), and using alternative fuels such as natural gas and hydrogen can be used to reduce emissions and improve engine performance [3–8]. Natural gas as an alternative fuel is considered in internal combustion engines due to its cleanliness. A study carried out to achieve high brake thermal efficiency and low methane (CH4) emissions in a natural gas–diesel dual fuel engine with a large–squish piston geometry. The results showed that the combination of an E–Pilot approach and a large–squish piston improve the BTE and CH4 emissions by indirect and direct injection with getting closer to the gasoline engine approach [9].

Improving engine power, torque and reducing engine emissions are very important. Therefore, researchers attempt to achieve these goals by changing engine geometry and using new methods [10,11]. Bayramoğlu and et al. [12] modeled a combustion chamber geometry so that a bowl geometry increase the air-fuel mixture quality with turbulence formation. The results were increase in engine performance and low emission.

In 1994 [13]. A study was carried out in the Gas Research Institute on a dual natural gas/diesel engine. The results showed that dual-fuel engine technology has many advantages such as high efficiency and brake mean effective pressure, significant reduction of nitrogen oxides (NOx), and particles. Other advantages of these engines are the economical use of fuel to obtain high-performance in applications like locomotive engines, marine engines, and trucks. For applying natural gas as an alternative fuel in a diesel engine, converting it into a spark-ignition engine was needed. Raine et al. [14] converted a diesel engine into a spark-ignition engine using natural gas fuel. In This conversion, the main engine characteristics were compression ratio, ignition timing, and fuel to air ratio. The compression ratio decreased from 1: 18 to 1: 15 and 1:13. The results of their study after a distance of 58,000 km on urban and suburban roads demonstrated that engine performance with a compression ratio of 1:15 was acceptable. Other studies have shown that in a diesel engine to use natural gas and hydrogen fuel, in addition to changing it to a gasoline engine, it is necessary to change other parameters such as the ignition timing [15].

In another study, the exhaust emissions of a turbocharged 1.8 lit 6-cylinder engine were investigated that converted into a gas-fired engine [16]. The results showed that the exhaust emissions were different at different loads. Meanwhile, NOx emission decreased so that CO, soot, and particles increased. Also, their concentration was significantly reduced by the oxidation catalyst.

The simulation and experimental results of diesel engine conversion into the natural gas engine at different speeds showed that fuel efficiency increased and, a significant

reduction in NOx and CO_2 emissions was observed [16]. The researchers [17–20] also showed that the use of the Wiebe single and double function combustion model in commercial diesel vehicles could help to improve the study of numerical and experimental methods so that the results indicated the acceleration of the predicting process of the optimal conditions with the least possible error.

A combination of natural gas and hydrogen fuel was used in spark ignition and compression combustion engines because of the high reaction speed of hydrogen fuel [21–24]. By Hairuddin et al. [20], a numerical study on the effect of blending hydrogen with natural gas in a homogeneous charge compression ignition engine showed that NOx and CO were reduced. Of course, the engine efficiency was increased by 13–16%. Experimental evaluation [25] of hydrogen enrichment in a dual-fueled CRDI diesel engine demonstrated a decrease in CO, HC, and increase in NOx emissions by 35%, 16%, and 13% and improve in BTE and BSEC by 28% and 20%, respectively. The results of experimental study on combustion stability and performance of hydrogen-enriched compressed natural gas of a free-piston linear generator showed an improved in engine performance when $\lambda = 1.4$ [26].

Adding hydrogen fuel to natural gas in spark-ignition and diesel engines investigated by engine testbed dynamometer. The results showed that the injection of HCNG fuel using a high-pressure injector and ignition timing at 32 BTDC increases cylinder pressure, brake thermal efficiency, and reduces NOx value [27]. Also, another research result showed that when methyl ester is added to the combination of hydrogen and natural gas in a diesel engine, unburn hydrocarbons were significantly reduced compared to NOx due to complete ignition [28].

In a numerical and experimental study [29], the effect of EGR with different pressures was investigated on combustion features, performance, and emissions of a commercial vehicle with hydrogen-enriched to natural gas. The results of other research on the effects of EGR and lean-burn on an HCNG diesel engine have shown that in the case of EGR, the peak pressure inside the cylinder decreases and, the amount of NOx with high-pressure EGR has the lowest value. It can also be concluded because of lower pressure and combustion rate. The thermal efficiency with EGR is lower than that without EGR under stoichiometric conditions [30]. EGR supply significantly affects the dual fuel engine combustion and emission levels. So that method of pilot fuel addition and EGR is affected dual fuel engine performance, but provided drastic reductions in smoke and NOx emissions [31].

The use of EGR indirect injection ignition engines with HCNG fuel showed that 5–10% of EGR could maintain engine efficiency under optimal conditions. In addition, the amount of NOx can be reduced by 25% EGR to 80% and keep the amount of carbon monoxide and unburned hydrocarbons in the low range [32]. The results of other studies on Butanol-gasoline (B20) and EGR gasoline engines have shown that EGR diluted with excess air improves braking thermal efficiency and produces lower amounts of NOx [33]. In general, the effect of EGR on diesel engines with HCNG fuel has a decreasing effect on NOx [34–36].

Today, one of the main topics in big cities is the reduction of exhaust emissions in internal combustion engines. Since the existence of EGR in internal combustion engines causes reduce harmful emissions to the environment, research in this area is necessary. However, the main point is that the EGR percentage added to cylinder inlet air is limited. In this study, a diesel engine was first converted to a gasoline engine and then optimized engine performance and exhaust emissions, the above items were investigated using AVL Fire multi-domain Simulation. The main variables were the combination of natural gas with hydrogen and the percentage of EGR ratio to the intake air in different cycles. The Gaussian process regression (GPR) was developed to model engine performance and exhaust emissions. The optimal values of EGR and the percentage of hydrogen in the blend of HCNG were extracted using a multi-objective genetic algorithm (MOGA). Finding the optimal point in terms of hydrogen content in fuel composition and EGR percentage using independent variables helps engine designers to maximize efficiency and reduce engine emissions. This issue has been less addressed in previous studies using both numerical and statistical methods by researchers.

Also, this point is significant that adding hydrogen to natural gas increases NO_X. One way to reduce NOx is to use EGR in internal combustion engines. However, in order to increase the efficiency and also to reduce the exhaust gases, it is necessary to completely target the optimal point for both the percentage of hydrogen in the blend of fuel and the amount of EGR. This issue has been investigated in this study.

Materials and methods

Engine studied and simulation conditions

The Perkins 1103A-33TG1 diesel engine is one of the ones widely used in the transportation and agricultural industries. The technical specifications of the studied engine are given in Table 1.

AVL Fire software was used to solve the combustion problem in this engine and simulated its process. Before the simulation, the geometry of the engine was designed and prepared. Then the engine mesh network was produced using Gambit. Since AVL Fire software only can analyze an organized network, this was done by connecting different blocks. In the simulation process, when the piston or valves move, the internal structure of the mesh changes automatically. Fig. 1 shows the geometry of the motor with the meshes created.

Network independence is a compelling issue in numerical solutions. Therefore, a numerical solution was performed with three networks and different numbers of cells. Then, to reduce the calculations, the closest number of networks that were slightly different from each other was selected.

Engine model

The engine model is a direct injection engine with the technical specifications of Table 1. The engine was converted from compression ignition to spark ignition and used a combination of natural gas and hydrogen fuel. Different EGRs were

Table 1 – Engine specification.

Engine	Perkins 1103A-33TG1		
Number of cylinders	3	Cycle	4 Stroke
Bore and Stroke (mm)	105 × 127	Length (cm)	104
Compression Ratio	17:1	Number of nozzle holes	4
Displacement (L)	3.3	Fuel mass	5.2 × 10-6 kg
Maximum Power	47kw	Nozzle hole diameter	0.0002 m
Aspiration	turbocharged	Start of injection	23° CA BTDC
Combustion system	Indirect injection	End of injection	7 °C A ATDC

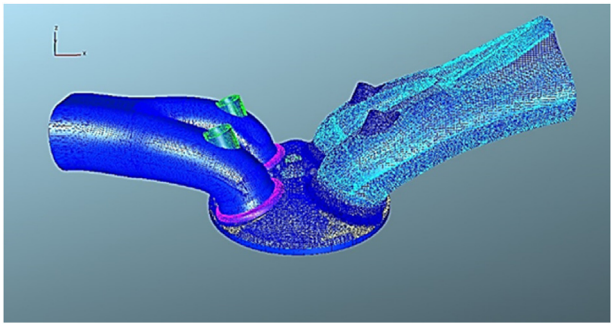

Fig. 1 – Piston set and Grid Solution Field.

used at different cycles to evaluate engine performance and exhaust emissions. In order to analyze the engine, different exhaust and air inlet ports were considered. Also, injection timing and ignition timing were considered so that the engine conditions could be correctly predicted. To simulate the engine, the engine geometry was plotted using actual sizes and the engine technical catalog by CATIA software and then meshed with Gambit software and the pentahedron method. The meshes were defined to include all points of the curve. The designated domain refinement algorithm was used for the in-cylinder mesh, the hydrogen and natural gas inlet boundary as the fuel used. The maximum selective tuberculosis at the lowest point of the cylinder, i.e., the bottom dead point, was 670,000 and the number of nodes was more than one million. Finally, the proposed model was transferred to AVL Fire software for numerical calculations.

Also, in this study, three types of fuels were used to evaluate the performance of the engine and exhaust pollutants. Due to the incomplete combustion of diesel fuel in the internal combustion engines and increased emissions, it can be replaced with natural gas and hydrogen fuel, which has very low pollution. However, to optimize engine performance, it is necessary to combine specific percentages of hydrogen fuel with natural gas. Some properties and characteristics of the fuels used are given in Table 2, [37–39].

Simulation model setup and validation

In this research, after converting the engine to spark ignition, the fuel changed from diesel to natural gas and then the mixture of natural gas and hydrogen with different percentages. It was used to evaluate the engine performance and exhaust gases under different EGR ratios. The combustion process and fluid flow inside the combustion chamber were simulated and some phenomena such as spray, droplet

Table 2 – Some properties of used fuels.

Property	methane	hydrogen	Diesel
Molecular weight (g/mol)	16.04	2.02	170
Density (kg/m^3)	0.65	0.08	800–840
Octane number	120	130	40-57 (Cetane Nu)
Auto ignition temperature (°C)	540	585	355
Mass diffusivity in air (cm^2/s)	0.16	0.61	0.0245
Minimum ignition energy (mJ)	0.28	0.02	0.16
Minimum quenching distance (mm)	2.03	0.64	5.5
Flammability limits in air (vol %)	5–15	4–75	0.79-5-54
Flammability limits (λ)	2–0.6	10–0.14	0.6
Flammability limits (φ)	5–1.6	0.1–7.1	1.32
Laminar burning velocity in air (m/s)	0.4	3.2	0.4
Lower heating value (MJ/kg)	50	120	36
Higher heating value (MJ/kg)	55.5	142	45.6
Stoichiometric air-to-fuel ratio (kg/kg)	17.1	34.2	15
Stoichiometric air-to-fuel ratio (kmol/kmol)	9.547	2.387	94.7

evaporation, and heat transfer were modeled. Due to the study of the flow inside the combustion chamber and the combustion process, the simulation was performed in a closed cycle so that the simulation was done from the inlet valve closing point to the outlet valve opening point. Also, due to the complexity of the chemical mechanism of natural gas and diesel, the chemical mechanism was used. The chemical reactions of combining both natural gas and hydrogen fuels are many numbers and the use of computational fluid dynamics codes is very time-consuming. Therefore, a reduced PRF mechanism including 77 species was used in this study. The Zeldovich mechanism developed in the cylinder was used to calculate NOX emissions in AVL Fire. The EGR module was used to model the EGR settings as the percentage of gas returned in the total mixture, including fresh air and inlet fuel, as in Formula 1.

$$EGR(\%) = \left(\frac{\dot{m}_{EGR}}{\dot{m}_{air} + \dot{m}_{fuel} + \dot{m}_{EGR}}\right) \times 100 \quad (1)$$

AVL fire simulation validation

Cylinder pressure and brake thermal efficiency are two main parameters in simulation validation. These are due to many engine parameters, including heat transfer and engine power, depending on cylinder pressure and thermal efficiency. The thermal efficiency of an engine indicates its high

Table 3 – Comparison of brake thermal efficiency for laboratory conditions [40] and simulated.

Brake thermal Efficiency (%)	Diesel	H_2 (2.5 gr/min) + Diesel	H_2 (2.5 gr/min) + Diesel with 10 EGR	H_2 (2.5 gr/min) + Diesel +With 20% EGR
0% Load	0[a] (0)	0 (0)	0 (0)	0 (0)
40% Load (kW)	19.5 (20.30)	22.5 (23.10)	21.8 (22.20)	20.4 (20.75)
80% Load (kW)	30.2 (31.30)	34 (34.71)	32.5 (33.10)	31.1 (31.8)

[a] Experimental data (Simulation data).

performance. Engine thermal efficiency at different loads at 1500 rpm was measured according to the amount of hydrogen-enriched in diesel fuel with 10% EGR and 20% EGR.

Here, Bose & Maji [40] laboratory results under similar conditions were used to validate the model built in AVL fire. The comparison results of brake thermal efficiency for different fuel conditions are given in Table 3. As can be seen, there is very little difference between the laboratory and simulated conditions, so it can be said that the simulated model is appropriately designed, and the prediction and calculations of the simulated model can be trusted. The parentheses in the table below show the simulation values. Also, a four-stroke single-cylinder engine with a stroke of 120 mm and a cylinder diameter of 80 mm was modeled to extract the simulation results. The maximum engine power was 5.2 kW and the compression ratio was 17.5: 1 (see Table 4 shows the amount of energy and mass in the HCNG blend).

Governing equations

The survival equation, the momentum equation, the energy equation, the species transfer equation, the turbulence equation, the combustion model, the emission equations, the air-to-fuel ratio equation, and the particle evaporation equations are some of the relationships discussed in simulating combustion engine combustion engines. Numerical discretization methods were used to solve the equations. The relationships entered to describe the fluid flow behavior in the solution field will be resolved in the Cartesian coordinate plane. If the velocity of the fluid flow in the center of the control volume is defined as a vector, the survival equation is expressed as follows:

$$-\frac{\partial V}{\partial t}=\frac{\partial(\rho u)}{\partial x}+\frac{\partial(\rho v)}{\partial y}+\frac{\partial(\rho w)}{\partial z} \tag{2}$$

Through the Navier-Stokes equation, the velocity and pressure of fluid flow change in different dimensions are interdependent.

Table 4 – The amounts of Energy and Mass in the HCNG blend.

	0% HCNG	10% HCNG	20% HCNG	30% HCNG	40% HCNG
H_2 (%Mass)	0	1.21	2.69	4.52	6.72
H_2 (%Energy)	0	3.09	6.68	10.49	15.59
LHV(MJ/kg)	46.28	47.17	48.26	49.61	51.41
CNG mass (mg)	5.2	5.13708	5.06012	4.96496	4.855
Hydrogen mass (mg)	0	0.6292	0.13988	0.23504	0.345

$$\hat{\rho}\frac{D\widehat{U_i}}{Dt}=\hat{\rho}\frac{\partial\widehat{U_i}}{\partial t}+\hat{\rho}\widehat{U_i}\frac{\partial\widehat{U_i}}{\partial x_j}=\hat{\rho}g_i+\frac{\partial\widehat{\sigma_{ij}}}{\partial x_j}=\hat{\rho}g_i-\frac{\partial\hat{P}}{\partial x_i}+\frac{\partial}{\partial x_j}\left[\mu\left(\frac{\partial\vartheta_i}{\partial x_j}+\frac{\partial\vartheta_j}{\partial x_i}-\frac{2}{3}\frac{\partial\vartheta_K}{\partial x_K}\delta_{ij}\right)\right] \tag{3}$$

where $\widehat{U_i}$ is the local velocity of the fluid flow, $\hat{\rho}$ is the density of the fluid flow, g_i is the acceleration of the earth's gravity, $\hat{P}$ is the pressure of the fluid flow, μ is the kinematic viscosity, ϑ_i and ϑ_j are the stress tensors between the fluid flow lines and δ_{ij} is the stress resulting from the interaction of the fluid flow with the wall of the solution field [41].

The enthalpy equation represents the combustion heat outputs, the heat near the walls, and the heat rate released, which affects the performance parameter of the indicator power. The energy equation can be represented as the following continuous polynomial:

$$\hat{\rho}\frac{D\hat{H}}{Dt}=\hat{\rho}\left(\frac{\partial\hat{H}}{\partial t}+\widehat{U_j}\frac{\partial\hat{H}}{\partial x_j}\right)=\hat{\rho}\dot{q_g}+\frac{\partial\hat{P}}{\partial t}+\frac{\partial}{\partial x_i}\left(\widehat{\tau_{ij}}\widehat{U_j}\right)+\frac{\partial}{\partial x_i}\left(\lambda\frac{\partial\hat{T}}{\partial x_j}\right) \tag{4}$$

$\hat{H}$ is the local enthalpy of the fluid flow, $\dot{q_g}$ is the heat exchange rate in the gaseous mixture, $\widehat{\tau_{ij}}$ is the shear stress between the fluid flow lines, λ is the fuel ratio and $\hat{T}$ is the fluid flow temperature [42].

Concerning species transfer, the exact amount of all species, how they mix, penetration and evaporation of the two fluid phases are stated. On describing the reaction kinetics of dual-fuel diesel engines, the behavior of the species at each stage of the reaction is estimated based on the species transfer relationship [43]:

$$\frac{\partial}{\partial t}(\rho Y_i)+\nabla(\rho\vec{v}Y_i)=-\nabla\vec{J_i}+R_i+S_i \tag{5}$$

where Y_i represents the input species, ϑ is the viscosity of the fluid flow, J_i indicates the infiltration of the species, R_i represents the rate of production of the species after the reaction, and S_i represents the source of the species created in the previous reaction and enters the new equation.

The air-to-fuel ratio in compression ignition engines determines whether the fuel mixture is rich or thin. The ratio of air to fuel stoichiometry in a turbocharged diesel engine is considered from 20:1 to 25:1. In the study, the ratio of air to fuel was considered stoichiometric 23:1 [44]:

$$AFR=\dot{m}_{gaseous\ fuel}.LHV_{gaseous\ fuel}/\dot{m}_{Diesel\ fuel}.LHV_{Diesel\ fuel}+\dot{m}_{gaseous\ fuel}.LHV_{gaseous\ fuel} \tag{6}$$

$\dot{m}_{\text{gaseous fuel}}$ and $\dot{m}_{\text{Diesel fuel}}$ are the mass flow rates of gaseous fuel and spray fuel, respectively. The ratio of gas fuel

Table 5 – Kernel function types used in this study to design a GPR model.

Kernel function	Equation
ARD Matern 3/2	$k(x_i, x_j\|\theta) = \sigma_f^2(1+\sqrt{3}r)\exp(-\sqrt{3}r),\ r = \sqrt{\sum_{m=1}^{d}\frac{(x_{im}-x_{jm})^2}{\sigma_m^2}}$
ARD Matern 5/2	$k(x_i, x_j\|\theta) = \sigma_f^2(1+\sqrt{5}r+\frac{5}{3}r^2)\exp(-\sqrt{5}r)$
Matern 3/2	$k(x_i, x_j\|\theta) = \sigma_f^2\left(1+\frac{\sqrt{3}r}{\sigma_l}\right)\exp(-\frac{\sqrt{3}r}{\sigma_l}),\ r = \sqrt{(x_i-x_j)^T(x_i-x_j)}$
Matern 5/2	$k(x_i, x_j\|\theta) = \sigma_f^2(1+\frac{\sqrt{3}r}{\sigma_l}+\frac{5r^2}{3\sigma_f^2})\exp(-\frac{\sqrt{5}r}{\sigma_l})$
ARD squared exponential	$k(x_i, x_j\|\theta) = \sigma_f^2 exp\left[-\frac{1}{2}\sum_{m=1}^{d}\frac{(x_{im}-x_{jm})^2}{\sigma_m^2}\right]$
Squared exponential	$k(x_i, x_j\|\theta) = \sigma_f^2 exp\left[-\frac{1}{2}\frac{(x_i-x_j)^T(x_i-x_j)}{\sigma_l^2}\right]$

ARD: automatic relevance determination.

to liquid fuel flow rate determines the volume percentage of fuels.

Chemical kinetics

Chemical equilibrium, as well as chemical kinetics, are capable of improving pollutant formation predictions from a SI engine. Although chemical equilibrium may qualitatively predict pollutant formation and emission from an engine, a chemical kinetics approach predicts the formation of pollutants in ICEs during the whole engine cycle, considering more coherent rates for each chemical species considered. Almost all chemical reactions require time for the entire set of reactions to ultimately happen. While some chemical compounds may react instantly, others may require considerable time to begin. For a one-step stoichiometric chemical reaction, the reactants and the products are represented based on the mass reaction law, Eq. (7)

$$\sum_{i=1}^{N}\acute{\upsilon}_i M_i = \sum_{i=1}^{N}\grave{\upsilon}_i M_i \tag{7}$$

where, $\acute{\upsilon}_i$ and $\grave{\upsilon}_i$: Stoichiometric Coefficients of the ith chemical species, related to the reactants and products, respectively; M_i : Specification of the molecule of the ith chemical species; N: Total number of chemical species on the model.

The rate of reaction of a specific chemical reaction is represented by Eq. (8).

Table 6 – R^2 values of GPR model based on different kernel functions in training, testing and total phase (for converting ppm to gr/kWh, it should be multiple at 1/100).

	Thermal efficiency (%)			Specific fuel consumption (gr/kW. h)		
Kernel function	Train	Test	Total	Train	Test	Total
Ardmatern32	**0.99 ± 0.00**	**0.99 ± 0.01**	**0.99 ± 0.00**	**0.99 ± 0.00**	**0.99 ± 0.01**	**0.99 ± 0.00**
Ardmatern52	0.99 ± 0.00	0.99 ± 0.01	0.99 ± 0.00	0.99 ± 0.00	0.99 ± 0.01	0.99 ± 0.00
Matern 32	0.99 ± 0.00	0.91 ± 0.02	0.97 ± 0.01	0.98 ± 0.00	0.95 ± 0.02	0.97 ± 0.01
Matern52	0.98 ± 0.00	0.92 ± 0.02	0.97 ± 0.01	0.98 ± 0.00	0.93 ± 0.03	0.96 ± 0.01
Ard squared exponential	0.99 ± 0.00	0.99 ± 0.01	0.99 ± 0.00	0.99 ± 0.01	0.99 ± 0.01	0.99 ± 0.01
Squared exponential	0.98 ± 0.00	0.92 ± 0.02	0.96 ± 0.01	0.98 ± 0.01	0.95 ± 0.02	0.97 ± 0.01
	Power output (kW)			NOx (ppm)		
Ardmatern32	**0.99 ± 0.00**	**0.99 ± 0.01**	**0.99 ± 0.00**	**0.99 ± 0.00**	**0.99 ± 0.01**	**0.99 ± 0.00**
Ardmatern52	0.99 ± 0.00	0.99 ± 0.01	0.99 ± 0.00	0.99 ± 0.00	0.98 ± 0.01	0.99 ± 0.00
Matern 32	0.99 ± 0.00	0.92 ± 0.03	0.98 ± 0.01	0.98 ± 0.00	0.98 ± 0.01	0.98 ± 0.00
Matern52	0.99 ± 0.00	0.92 ± 0.03	0.98 ± 0.01	0.99 ± 0.01	0.99 ± 0.01	0.99 ± 0.01
Ard squared exponential	0.99 ± 0.00	0.99 ± 0.01	0.99 ± 0.00	0.99 ± 0.01	0.98 ± 0.01	0.99 ± 0.01
Squared exponential	0.99 ± 0.00	0.93 ± 0.02	0.98 ± 0.01	0.98 ± 0.00	0.98 ± 0.02	0.98 ± 0.01
	CO (ppm)			HC (ppm)		
Ardmatern32	**0.99 ± 0.00**	**0.99 ± 0.01**	**0.99 ± 0.00**	**0.99 ± 0.01**	**0.98 ± 0.02**	**0.99 ± 0.01**
Ardmatern52	0.99 ± 0.00	0.99 ± 0.01	0.99 ± 0.00	0.99 ± 0.01	0.97 ± 0.02	0.99 ± 0.01
Matern 32	0.99 ± 0.00	0.99 ± 0.01	0.99 ± 0.00	0.99 ± 0.01	0.96 ± 0.03	0.99 ± 0.01
Matern52	0.99 ± 0.00	0.99 ± 0.01	0.99 ± 0.00	0.99 ± 0.01	0.96 ± 0.03	0.98 ± 0.01
Ard squared exponential	0.99 ± 0.00	0.99 ± 0.01	0.99 ± 0.00	0.99 ± 0.01	0.97 ± 0.02	0.99 ± 0.01
Squared exponential	0.99 ± 0.00	0.99 ± 0.01	0.99 ± 0.00	0.99 ± 0.01	0.97 ± 0.02	0.99 ± 0.01

$$RR = \frac{dC_p}{dt} = \frac{dC_R}{dt} = k\prod_{i=1}^{N} C_i^{\acute{v}_i}$$

$$RR = \frac{dC_p}{dt} = \frac{dC_R}{dt} = k\prod_{i=1}^{N} C_i^{\acute{v}_i} \quad (8)$$

where, RR: Reaction Rate; k: The Rate Constant of the chemical reaction; C_p and C_R: Molar concentration of the products or reactants respectively $\left(\frac{kmol}{m^3}\right)$; C_i: Molar concentration of the chemical species $\left(\frac{kmol}{m^3}\right)$;

The overall chemical of the HCNG blend with different hydrogen volumetric concentration is presented in Table 3.

Gaussian process regression (GPR) model

Due to the need to use software such as AVL fire, to simulate the combustion conditions of the engine understudy requires almost heavy calculations, as mentioned earlier. Therefore, EGR was used to obtain the graph of the engine performance response level in terms of fuel composition, and GPR for different engine speeds in this research. Thus, the designed

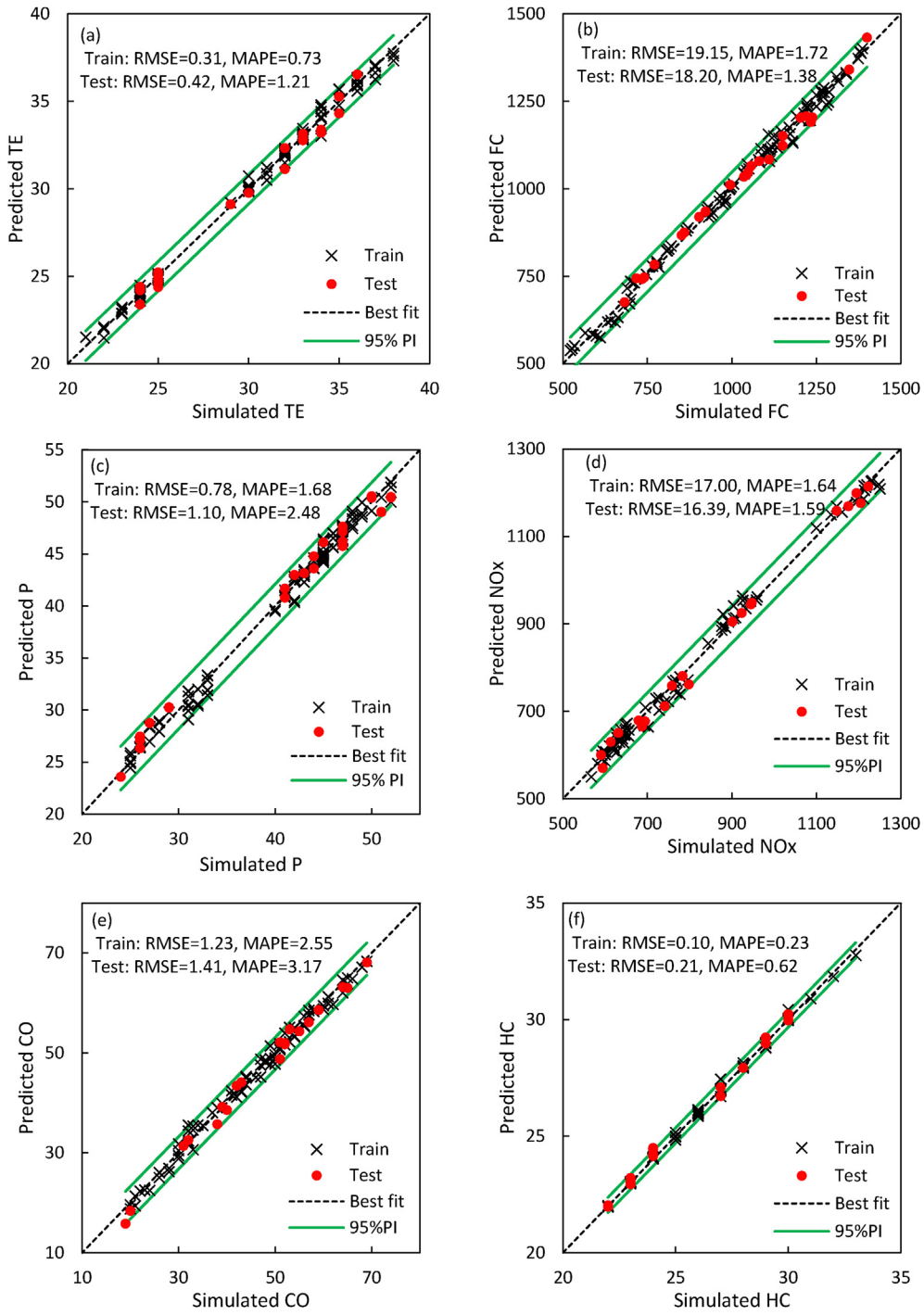

Fig. 2 – The result of evaluating the agreement between the simulated data set with the data set predicted by GPR.

GPR model can be replaced for heavy software and in the following, it can be used as a cost function in the genetic algorithm. The GPR modeling is based on a stochastic process in which a set of random variables with a Gaussian distribution is created [45]. The Gaussian process (GP) is a function of mean (m (x)) and covariance (kernel) function (k (x, x′)). The GP function is defined as Eq. (9):

$$t(x) \sim GP(m(x), k(x, x')) \tag{9}$$

The purpose of the GPR model is to generate the relationship between the response variable (y) and predictor variables (x_i) according to Eq. (9). In this study, response variables include thermal efficiency, fuel consumption, power output, NOx, CO, HC and predictor variables including EGR, HCNG, and engine speed. ε in this equation refers to the model error. In addition, it is a factor with an independent identically distributed Gaussian property, i.e. $\varepsilon \sim N(0, \sigma_n^2)$

$$y = t(x) + \varepsilon \tag{10}$$

Assuming we have an identity matrix (I), Eq. (9) can be rewritten as Eq. (10).

$$t(x) \sim GP(m(x), k(x, x') + I\sigma_n^2) \tag{11}$$

By dividing the available data set into two training data sets (X, y) and a set of test data (X_*, f_*) [46]:

$$\begin{bmatrix} y \\ f_* \end{bmatrix} \sim \left(\begin{bmatrix} m(X) \\ m(X_*) \end{bmatrix}, \begin{bmatrix} k(X, X') + I\sigma_n^2 & k(X, X_*) \\ k(X_*, X) & k(X_*, X_*) \end{bmatrix} \right) \tag{12}$$

Proper selection of the Kernel function type (KF) is essential in GPR modeling. The success of GPR training and its generalizability in the testing phase depends on the appropriate choice of KF. Various types of KFs have been used in various sources. In this study, based on practical experience of the leading problem and the results of others [47,48], six types of KF were used (Table 5). In this table, σl refers to the signal variance of function and length scale, respectively.

The parameters of the functions m (x) and k (x, x') are calculated using a randomly selected training dataset. The set of these parameters is called hyper parameters (θ). The quasi-Newton approximation to the Hessian (QNAH) training algorithm was used to find the optimal values of vector θ. This algorithm is based on the conjugate method gradient that has been established [49].

Since the unit and vector scale of the motor variables (x) were different from each other, and also in order to improve the training process, the data were first normalized using Equation (5) at intervals [-1,1] (x_n):

$$x_n = 1 + \frac{2(x - x_{min})}{(x_{max} - x_{min})} \tag{13}$$

where, x_{max} and x_{min} are the maximum and minimum values of the input vector (x).

MATLAB software was used for modeling and data analysis.

Results and discussion

As described in the section of materials and methods, six types of kernel functions were used to design the GPR model. The mean values and standard deviation R^2 of the model ($\bar{R}^2 \pm std$) in estimating the six performance criteria of the engine are given in Table 6. These results were obtained using 5-fold with 20 replications. Therefore, the prediction results were obtained based on 100 different arrangements of the total simulated data. Accordingly, the closer the mean is to one and the standard deviation to zero, the model has a high ability to replace the simulated model of AVL fire and has better generalizability. Based on the explanations given and the results of Table 6, the use of ARD Matern 3/2 as a kernel function in the GPR model leads us to the best possible result in this research. The average value of R^2 for thermal efficiency, fuel consumption, power output, NOx, CO and HC is 0.99. This means that the designed GPR model can be used with 99% confidence to replace the simulated model. In addition, the small value of standard deviation R^2 indicates the fact that the GPR model has very good generalizability.

Fig. 2 shows the RMSE and MAPE values and the agreement between the two simulated data sets of engine performance versus their values predicted by the GPR designed model. As can be seen, the GPR model can predict the engine performance parameters with a maximum error of about 3%. Also, the RMSE values for thermal efficiency, fuel consumption,

Table 7 – Assessment of generalizability capability of the GPR model .

	Thermal efficiency (%)						Specific fuel consumption (gr/kW. h)					
	Train		Test		Total		Train		Test		Total	
	R^2	RMSE	R^2	RMSE	R^2	RMSE	R^2	RMSE	R^2	RMSE	R^2	RMSE
80	0.99	0.31	0.99	0.42	0.99	0.34	0.99	19.15	0.99	18.20	0.99	18.96
60	0.99	0.32	0.99	0.40	0.99	0.35	0.99	18.75	0.99	20.32	0.99	19.40
40	0.99	0.31	0.97	0.76	0.98	0.62	0.99	18.50	0.99	21.91	0.99	20.62
	Power output (kW)						NOx (ppm)					
80	0.99	0.78	0.99	1.10	0.99	0.85	0.99	17.00	0.99	16.39	0.99	16.88
60	0.99	0.72	0.99	1.07	0.99	0.88	0.99	16.00	0.99	18.13	0.99	16.88
40	0.99	0.68	0.99	1.01	0.99	0.90	0.99	15.60	0.99	18.97	0.99	17.70
	CO (ppm)						HC (ppm)					
80	0.99	1.23	0.99	1.41	0.99	1.27	0.99	0.10	0.99	0.21	0.99	0.13
60	0.99	1.26	0.99	1.33	0.99	1.29	0.99	0.05	0.97	0.52	0.99	0.33
40	0.99	1.28	0.99	1.37	0.99	1.34	0.99	0.07	0.96	0.56	0.98	0.44

power output, NOx, CO and HC are 1.41, 16.39, 1.10, 18.20, 0.42, and 0.39, respectively. In addition, as can be seen, the dispersion of engine performance parameter data is compared to the best fit line between the two PI lines with a 95% probability. Therefore, based on this result, it can be said that there is very little difference between the results of the GPR model and AVL fire, and therefore the use of GPR instead of AVL fire is recommended. Indeed, replacing the GPR model as an agile model with high-speed calculation capability against the AVL fire model as a method with heavy calculations can be justified. Also, as described in Table 3 and Section AVL Fire Simulation Validation, the validity of the AVL fire simulation is discussed and validated. Now, according to the purpose of this study, the GPR model should be replaced with complex calculations and time-consuming AVL fire. Therefore, the prediction validity of the GPR model must be confirmed. Based on the results of Fig. 2, the maximum prediction error of the GPR model is less than 3%. In addition, as can be seen, the values predicted by the GPR model are around the 45-degree line (Best fit: y = x) and the 95% confidence interval confirms, so that the GPR model predictions have a probability of at least 95% with the AVL fire computing range. Therefore, the predictions of the GPR model as an alternative to AVL fire software can be trusted.

For better and more evaluation, the GPR model was changed as an alternative to AVL fire, the size of the training

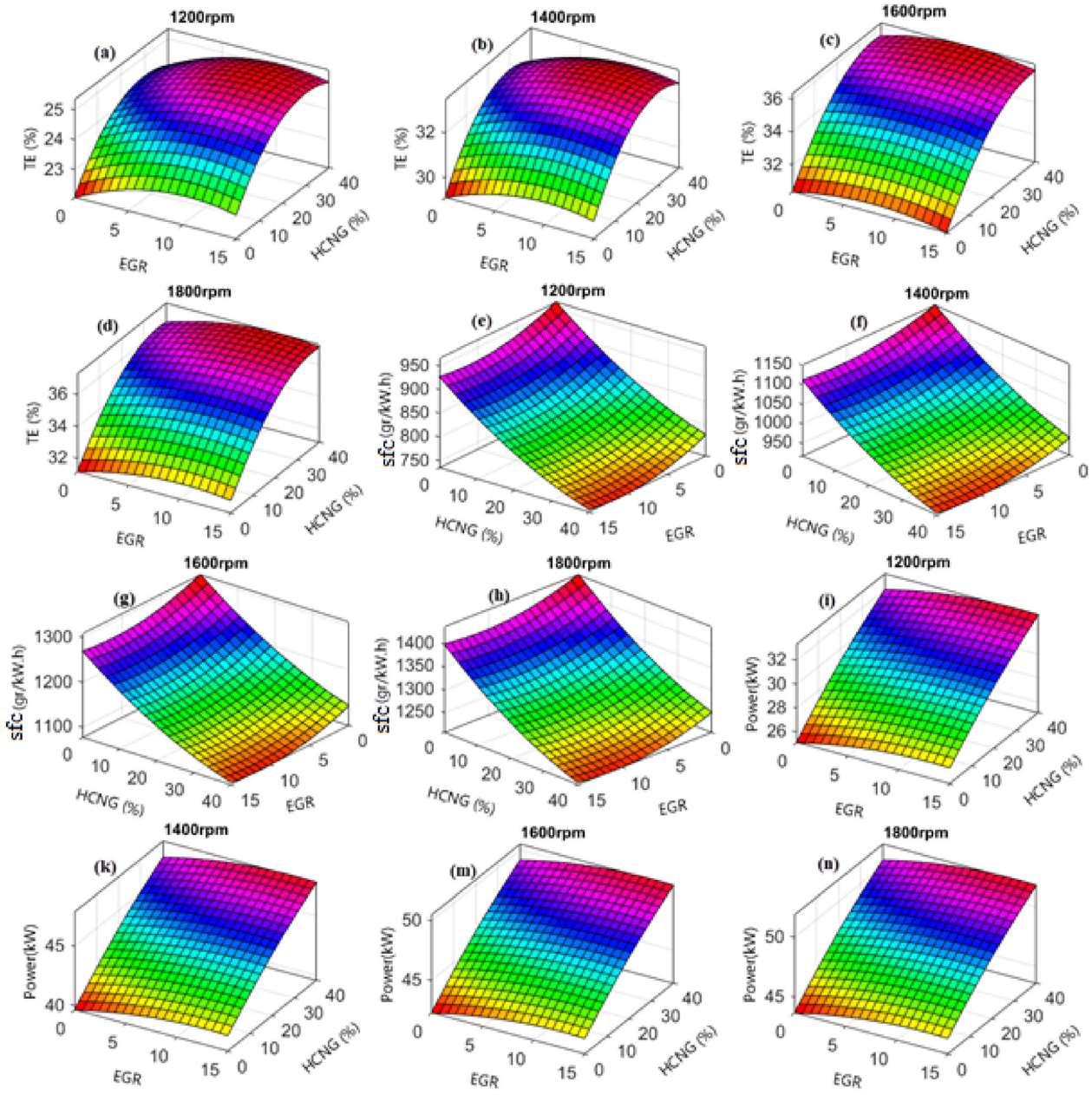

Fig. 3 – The Response Level of GPR Performance Parameters for Thermal Efficiency (TE), Specific fuel consumption (SFC), Power at 1200, 1400, 1600, 1800 rpm.

set. The results of this study are presented in Table 7 for six engine performance parameters for the training set size of 80, 60 and 40% random of the total simulated data set in three stages of training, testing and total. The reduction of the training set size makes the model have less learning experience in the training phase [50] and also, the model will face more new conditions with the increase of the test data set. Suppose the results of the model predictions with a smaller training data set are acceptable in both training and testing. Based on the explanations given in the results of Table 6 and the changes in R2, RMSE, by reducing the size of the training data set from 80% to 40%, it can be hoped that the GPR model has a very good generalizability. Therefore, a suitable model of engine behavior in the face of changes in parameters such as EGR, H_2, and RPM can be achieved with less computational volume in AVL fire.

Figs. 3 and 4 show the response level of changes for thermal efficiency (TE), NOx, CO, HC, specific fuel consumption (FC), power at 1200, 1400, 1600, 1800 rpm with the designed GPR model, respectively. By the response level, changes in engine performance can be observed against changes in the percentage of H_2 and EGR. It is noteworthy that it can be concluded that the amount of hydrogen in HCNG has a more significant effect on engine performance parameters than EGR by examining the slope of changes in engine performance parameters versus changes in HCNG and EGR because the

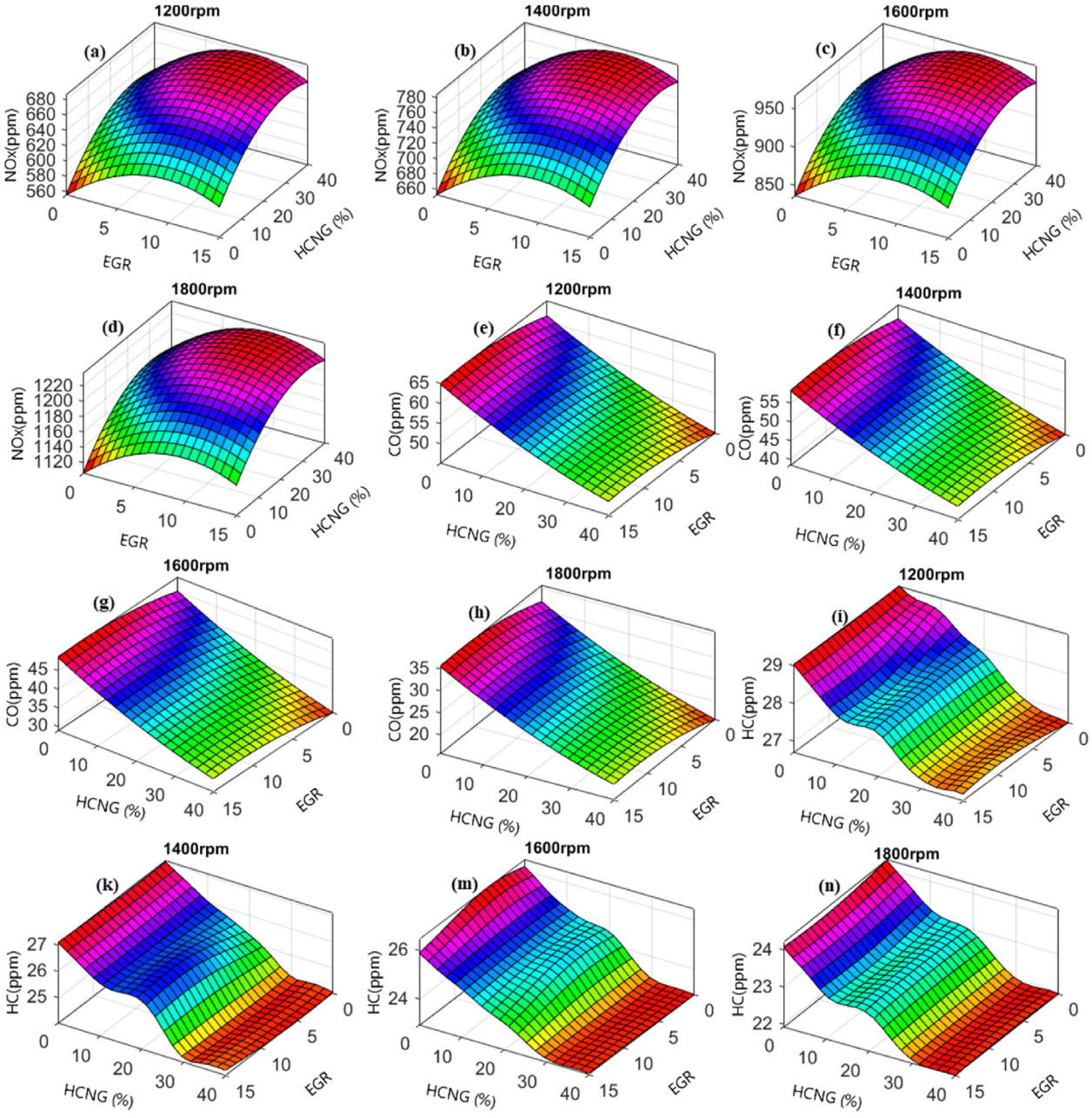

Fig. 4 – The Response Level of GPR Engine Emission Parameters for NOx, CO, HC at 1200, 1400, 1600, 1800 rpm (for converting ppm to gr/kWh, it should be multiple at 1/100).

Table 8 – The result of multi-objective optimization using genetic algorithm for different engine speeds.

EGR	%HCNG	rpm	TE (%)	FC (gr/kW. h)	P (kW)	NOx (ppm)	CO (ppm)	HC (ppm)
5.54	30.76	1000	24.96	582.50	30.11	648.01	53.87	28.83
5.83	30.81	1200	25.01	785.12	31.66	669.68	50.65	26.96
6.22	30.00	1400	33.31	961.72	46.15	775.17	44.70	24.11
5.63	32.20	1600	36.51	1108.64	48.96	953.62	33.85	23.02
8.43	31.24	1800	37.73	1228.24	50.52	1226.20	21.91	21.98
11.06	38.18	1000	25.03	543.61	31.58	–	–	–
11.59	36.15	1200	25.18	754.70	32.84	–	–	–
11.68	36.96	1400	33.28	929.26	47.40	–	–	–
11.30	37.74	1600	36.44	1077.28	50.14	–	–	–
11.82	37.50	1800	37.43	1202.47	51.58	–	–	–
0.05	24.14	1000	–	–	–	605.50	53.46	29.33
0.02	25.55	1200	–	–	–	626.89	49.62	27.21
1.67	26.66	1400	–	–	–	743.90	43.69	24.68
0.00	26.67	1600	–	–	–	912.10	32.92	23.42
0.07	25.47	1800	–	–	–	1175.97	20.41	22.36

slope of changes against HCNG will be significantly higher than EGR.

Based on Fig. 3 (a, b, c, d), it can be concluded that the maximum value of thermal efficiency at different engine speeds is about 10% for EGR and about 30% for HCNG. According to Fig. 3 (e, f, g, h), the minimum specific fuel consumption at different engine speeds is about 10% for EGR and 40% for HCNG. The results of Fig. 3 (i, k, m, n), the maximum amount of power at different engine speeds for EGR is about zero percent and HCNG about 40%. Therefore, thermal efficiency, engine power and also specific fuel consumption increase with low EGR and decrease with high EGR. High EGR increases the duration of combustion [51] so that this reduces the maximum production pressure in the combustion chamber and thus reduces engine power [52].

Based on Fig. 4 (a, b, c, d), the minimum NOx value at different engine speeds for EGR and HCNG is zero. The value of NOx increases with increasing combustion chamber

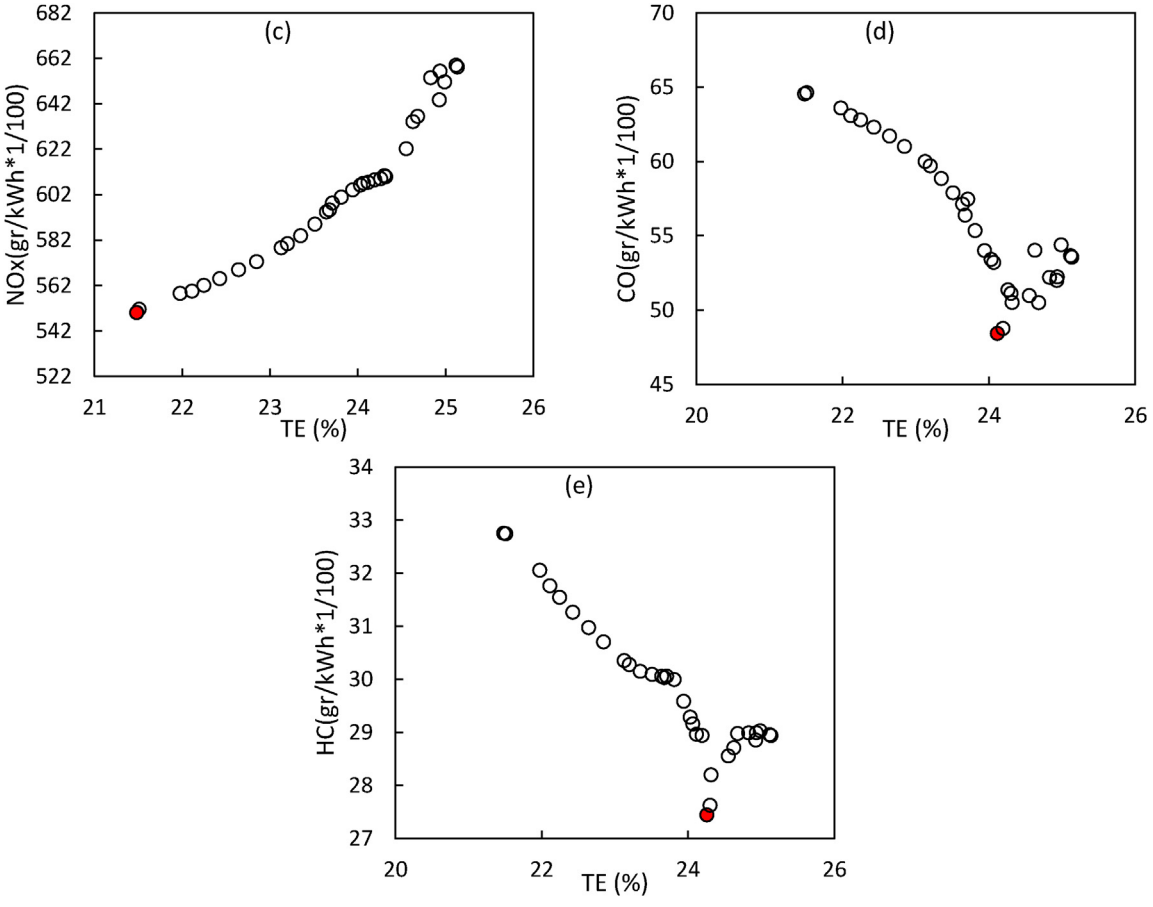

Fig. 5 – TE beam diagram versus other Engine performance parameters for 1000 rpm, red dot optimum combination selected from EGR and HCNG

temperature [53]. Due to the high rate of reaction of hydrogen fuel in the combustion chamber, high EGR and increasing the amount of hydrogen in the HCNG composition causes an increase in temperature which results in an increase in NOx [54,55]. Based on Fig. 3 (e, f, g, h), the minimum amount of CO at different engine speeds in EGR is about zero percent and HCNG is about 40%. The results of Fig. 4 (i, k, m, n), the maximum amount of HC at different engine speeds for EGR is about 0% and HCNG is about 40%. Reducing CO and HC emissions by increasing hydrogen is due to complete combustion so that with the increase of hydrogen in the fuel composition, it is possible to increase the temperature and also the higher pressure, and as a result, fewer emissions and more power [56].

As shown in the response level study (Figs. 3 and 4), the optimal value of each of the engine performance parameters were obtained in different values of EGR and HCNG, which were inconsistent with each other. Therefore, the appropriate multi-objective optimization method was used. Table 8 shows the optimal values of EGR and HCNG at different engine speeds using a multi-objective genetic algorithm. Three scenarios for optimization including multi-objective optimization based on six performance goals, multi-objective optimization based on three performance goals including TE, FC, Power and multi-objective optimization based on three objectives of reducing engine emissions were defined. As the results show, the optimal values of EGR and HCNG are different in different cycles. The optimal value of EGR in

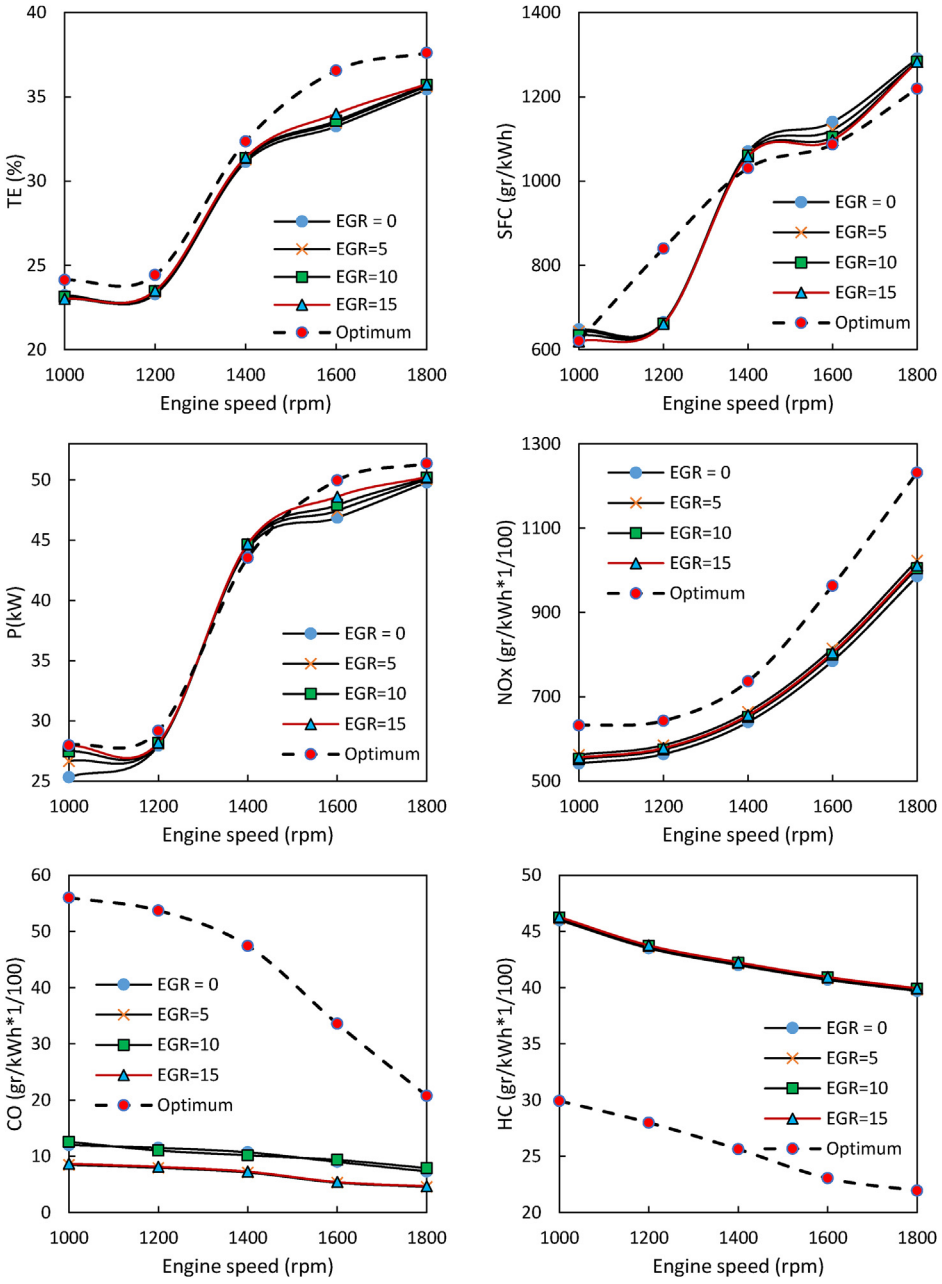

Fig. 6 – Curve of performance parameters and engine exhaust emissions versus engine speed for EGR percentage and also curve of optimum value for diesel fuel.

different cycles in the first scenario (optimization of all engine parameters) varies from 5.54 to 8.43 and for HCNG from 30.00 to 32.20, respectively. Also, the average optimal values of EGR and HCNG for all cycles are 6.53 and 31.00, respectively. Regardless of the engine emission performance, for the second scenario, i.e., the optimization of the three performance parameters TE, FC, Power, the optimal value of EGR in different cycles varies from 11.06 to 11.82 and for HCNG from 36.15 to 38.18. Also, the average optimal values of EGR and HCNG for all cycles are 11.49 and 37.31, respectively. The optimization of the engine emission parameters without considering TE, FC, Power (third scenario) showed that the optimal value of EGR at the lowest value (average 0.36) and the use of HCNG at an average value of 25.70 was the best result for engine emission. Fig. 5 shows the beam diagram of the changes in the optimal values of possible solutions for TE versus other engine performance variables for 1000 rpm. Therefore, based on the optimal conditions of EGR and HCNG in different cycles, the best value for the performance parameters a, b and the emission values of c-e can be obtained according to the thermal efficiency of TE.

One of the aims of this study is to optimize and find the optimal value of EGR in different periods based on the percentage of hydrogen to natural gas to reduce engine emissions and increase engine performance. Because the optimal value of percentage of hydrogen to natural gas is about 30%, therefore, based on 30% HCNG, the optimal value in different percentages of EGR can be obtained. Fig. 6 shows the curve of performance parameters and engine exhaust emissions versus engine speed based on the percentage of EGR and the graph of the optimum value for diesel fuel. Due to the reduction in combustion delay, the values of thermal efficiency and engine power increase, especially at high speeds with increasing EGR in a diesel engine [57], but the value of specific fuel consumption decreases so that at higher speeds, i.e., about 1600 rpm, the value decreases more intensively.

One of the most effective ways to reduce NOx pollutants is to use EGR. In this system, some of the exhaust gases are returned to the cylinder. This value of return exhaust gas enters the engine cylinder with the air in the suction course and plays the role of diluting the mixture together with the gases remaining from the previous cycle (O_2 reduction). As a result of this mixture, flame speed and peak combustion temperature decrease. Also, the value of NOx decreases. Therefore, due to less oxygen accumulation and lower flame temperature, the value of NOx decreases with increasing EGR [58] according to the following diagrams. Due to the complete combustion of the value of fuel inside the combustion chamber, the value of HC and CO also decreases with increasing EGR, but the value of HC decreases slightly. Finally, according to the statistical results extracted for diesel fuel with different EGRs, the results showed that the best engine performance and exhaust emissions with 10% EGR in different cycles could be achieved.

Fig. 7. Shows the variation of cylinder pressure versus crank angle at 1500 RPM. The following figure demonstrates that by increasing the EGR ratio, the amount of cylinder pressure decreases but the amount of reduction is very small. The cause of the reduction in cylinder pressure is the reduction of oxygen availability and the reduction of the fuel burning rate in the diffusion phase [59]. Also if in this case, as HCNG percentage in the blend of fuel increases, the cylinder

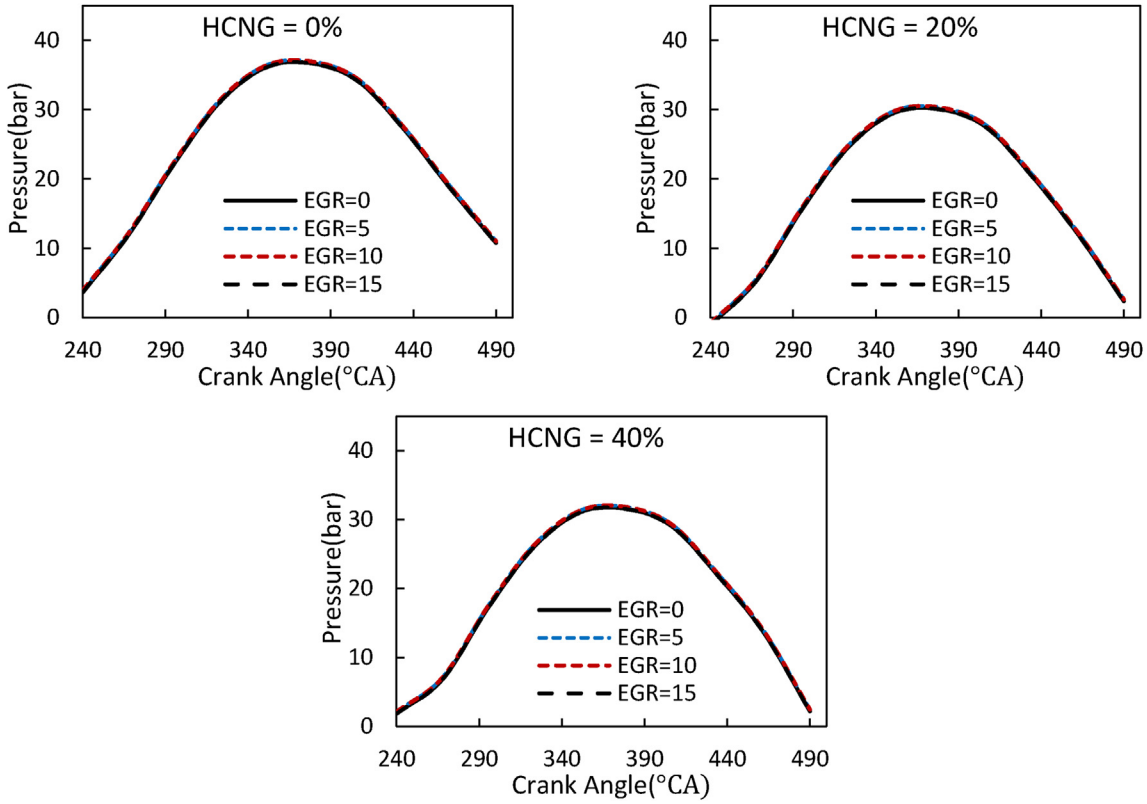

Fig. 7 – Variation of cylinder pressure versus crank angle at 1500 RPM.

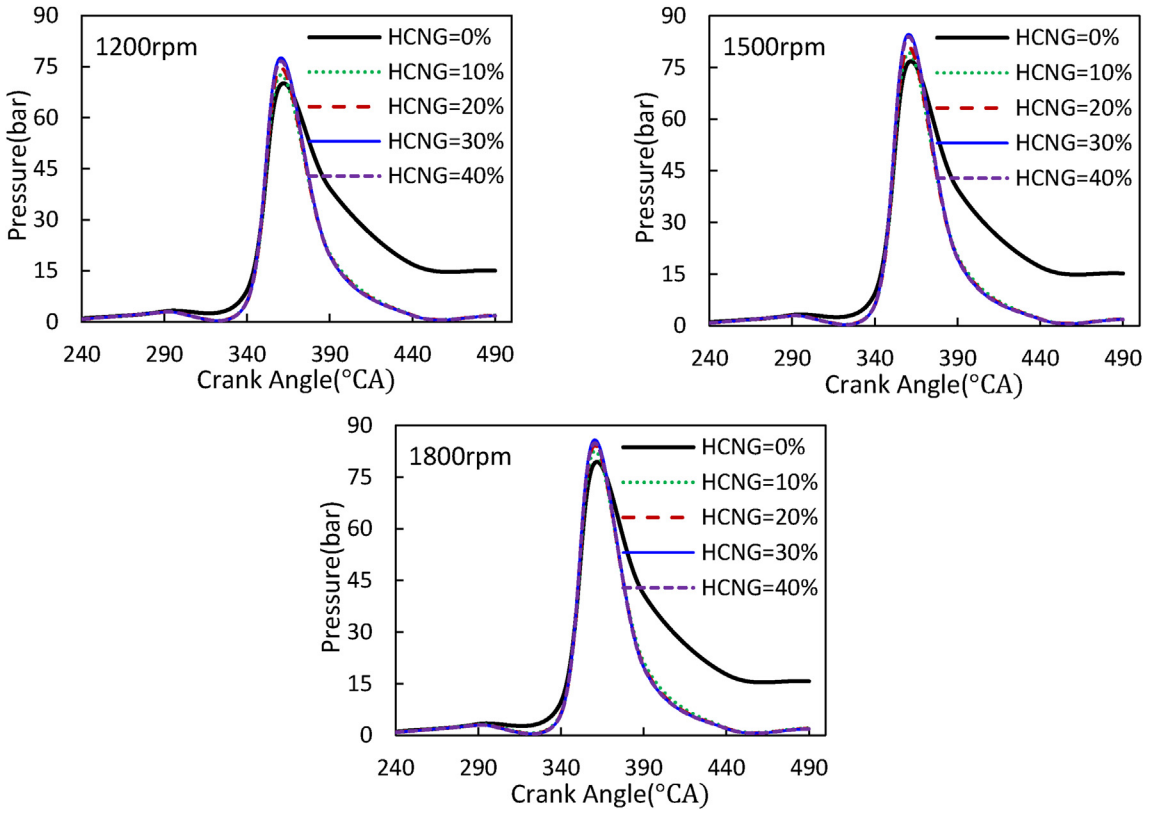

Fig. 8 – Variation of cylinder pressure versus crank angle at different engine speeds.

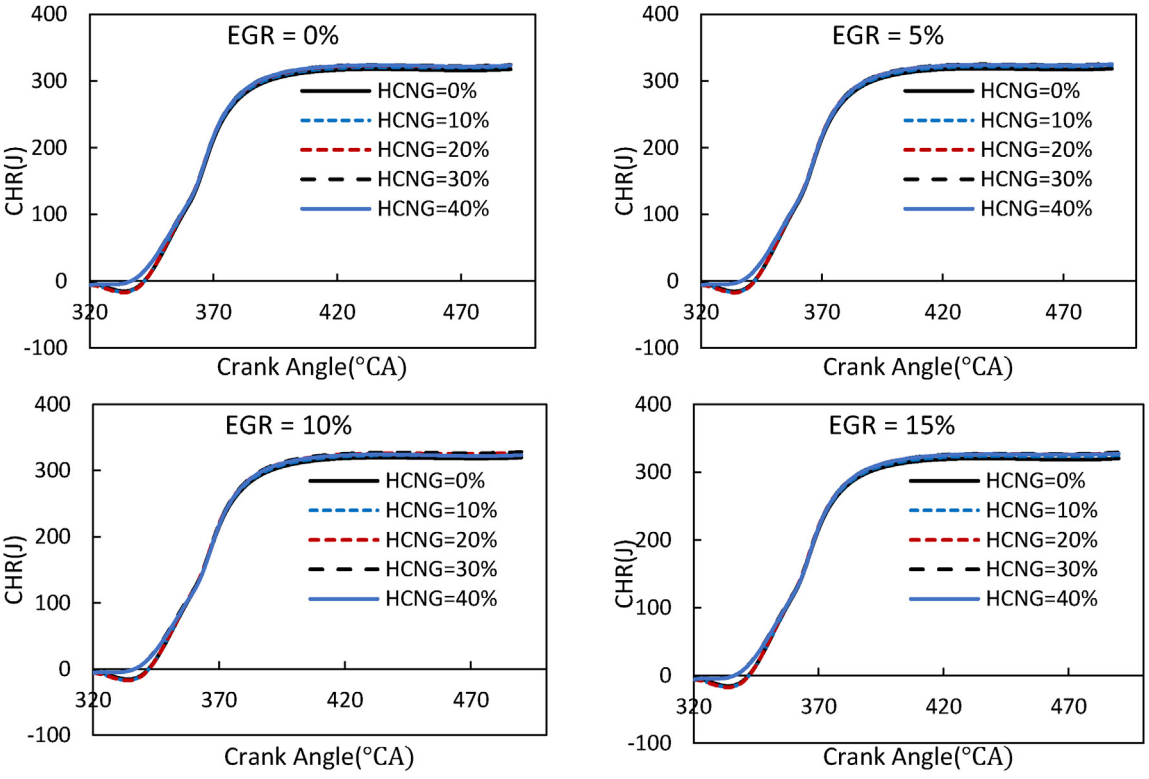

Fig. 9 – Variation of cylinder pressure versus crank angle at 1500 RPM.

pressure decreases. Meanwhile this point should be mentioned that at other engine speeds, the pressure trend is the same.

Fig. 8 shows that with an increase of hydrogen percentage in HCNG and engine speed, the cylinder pressure increases so that the curve of cylinder pressure generally is closed to top dead center [60] and this subject help to increase performance and engine efficiency due to the presence of further force when piston moves toward bottom dead center. Off course, as mentioned before, the maximum efficiency obtained is approximately at 30%HCNG because when the hydrogen percentage is more than this amount, the maximum cylinder pressure is closed to the top dead center and the pressure drops as the piston moves down.

Fig. 9 shows the variation of cylinder pressure versus crank angle at 1500 RPM. As can be seen due to the variation of hydrogen content in HCNG fuel, the increase of EGR ratio leads to the decrease of CHR, while when the EGR ratio reaches 15%, the CHR start to an increase due to increase of heat transfer in engine and cylinder wall. Meanwhile increase of hydrogen in HCNG blend more than 30% lead to decrease of combustion duration and finally decrease of the engine efficiency [61,62].

Conclusions

Although diesel cars play a pivotal role in freight and passenger transport, they are also considered a source of pollution. In this study, a diesel engine was simulated for investigating performance and exhaust emissions with a combination of natural gas and hydrogen fuel. Gaussian process regression (GPR) applied to model engine performance. Subsequently, the optimal values of the EGR ratio and the percentage of hydrogen were extracted at different speeds using a multi-objective genetic algorithm (MOGA). The following results were obtained from this investigation.

An evaluation of the GPR model showed that using the ARD Matern 2/3 as a Kernel function can be used with confidence to replace the AVL Fire simulation model.

The GPR model can replace the simulated model with 99% confidence. The comparison of the results predicted by the GPR and simulation model showed that the maximum error of the GPR model was about 3%. Also, the results of the GPR showed that the volume of calculations in AVL Fire significantly reduced against parametric changes of EGR, H2%, and RPM.

A Gaussian process regression model predicted the response level of performance and exhaust emissions at different engine speeds against HCNG and EGR values. The results showed that the highest value of thermal efficiency ratio to different engine speeds was obtained with 10% EGR and 30% EGR, while the lowest specific specific fuel consumption resulted with 10% EGR and 40% HCNG.

Thermal efficiency, engine power, and specific specific fuel consumption increased with decreasing EGR ratio. A high EGR ratio increases the combustion duration and thus reduces the pressure inside the combustion chamber.

Increase of EGR ratio on cylinder pressure had an insignificant effect but increase of hydrogen percentage in the fuel blend from 0% to 40% increased cylinder pressure about 9% at different engine speeds. Also increase of more than 10% EGR along with HCNG percentage lead to that cumulative heat release increase insignificantly.

Increasing the percentage of hydrogen in the fuel composition and the EGR ratio increases the combustion temperature and consequently increases the NOX, while the amount of CO and HC decreases. The lowest NO_X value was obtained with 30%HCNG and 10% EGR. Similarly, the lowest amount of CO and HC was obtained with 15%EGR. While, if the amount of hydrogen and EGR are used in combination, the lowest of them is obtained with 30%HCNG and 10%EGR.

According to the multi-objective optimization by genetic algorithm, the optimal values of EGR and HCNG based on maximum performance and minimum engine emissions are 6.35% and 31%, respectively.

One general conclusion is that, although hydrogen has a significant potential for emissions reductions, it is also experiencing very rapid growth in the petroleum refining industry.

Declaration of competing interest

The authors declare that they have no known competing financial interests or personal relationships that could have appeared to influence the work reported in this paper.

REFERENCES

[1] Lloyd AC, Cackette TA. Diesel engines: environmental impact and control. J Air Waste Manag Assoc 2001 Jun 1;51(6):809–47.
[2] Burtscher H. Physical characterization of particulate emissions from diesel engines: a review. J Aerosol Sci 2005 Jul 1;36(7):896–932.
[3] Chen H, Shi-Jin S, Jian-Xin W. Study on combustion characteristics and PM emission of diesel engines using ester–ethanol–diesel blended fuels. Proc Combust Inst 2007 Jan 1;31(2):2981–9.
[4] Sathiyagnanam AP, Saravanan CG, Gopalakrishnan M. Hexanol-ethanol diesel blends on DI-diesel engine to study the combustion and emission. Proc WRI World Congr Comput Sci Inf Eng 2010 Jun 30;2:1–5.
[5] Azizb A. PM emission of diesel engines using ester-ethanol-diesel blended fuel. Procedia Eng 2013;53:530–5.
[6] Heydari-Maleney K, Taghizadeh-Alisaraei A, Ghobadian B, Abbaszadeh-Mayvan A. Analyzing and evaluation of carbon nanotubes additives to diesohol-B2 fuels on performance and emission of diesel engines. Fuel 2017 May 15;196:110–23.
[7] Ahmadipour S, Aghkhani MH, Zareei J. Investigation of injection timing and different fuels on the diesel engine performance and emissions. J Comput Appl Res Mech Eng 2020 Feb 1;9(2):385–96.
[8] Jamrozik A, Grab-Rogaliński K, Tutak W. Hydrogen effects on combustion stability, performance and emission of diesel engine. Int J Hydrogen Energy 2020 Jul 31;45(38):19936–47.
[9] Park H, Shim E, Lee J, Oh S, Kim C, Lee Y, Kang K. Large–squish piston geometry and early pilot injection for high efficiency and low methane emission in natural gas–diesel dual fuel engine at high–load operations. Fuel 2022 Jan 15;308:122015.
[10] Zareei J, Kakaee AH. Study and the effects of ignition timing on gasoline engine performance and emissions. European Transport Res Review 2013 Jun 1;5(2):109–16.

[11] Zareei J, Rohani A. Optimization and study of performance parameters in an engine fueled with hydrogen. Int J Hydrog Energy 2020 Jan 1;45(1):322–36.
[12] Bayramoğlu K, Yılmaz S. Emission and performance estimation in hydrogen injection strategies on diesel engines. Int J Hydrog Energy 2021 Aug 18;46(57):29732–44.
[13] Raine RR, Stephenson J, Elder ST. Characteristics of diesel engines converted to spark ignition operation fuelled with natural gas. SAE Technical Paper; 1988 Feb 1.
[14] Mittal M, Donahue R, Winnie P, Gillette A. Exhaust emissions characteristics of a multi-cylinder 18.1-L diesel engine converted to fueled with natural gas and diesel pilot. J Energy Inst 2015 Aug 1;88(3):275–83.
[15] Luo H, Chang F, Jin Y, Ogata Y, Matsumura Y, Ichikawa T, Kim W, Nakashimada Y, Nishida K. Experimental investigation on performance of hydrogen additions in natural gas combustion combined with CO2. Int J Hydrog Energy 2021 Oct 11;46(70):34958–69.
[16] Liu J, Dumitrescu CE. Single and double Wiebe function combustion model for a heavy-duty diesel engine retrofitted to natural-gas spark-ignition. Appl Energy 2019 Aug 15;248:95–103.
[17] Likhanov VA, Rossokhin AV. The impact of the use of compressed natural gas in a car diesel engine on the formation and oxidation of soot particles. InIOP Conference Series: Mater Sci Eng 2020 Jan;734(1):12207. IOP Publishing.
[18] Liu J, Dumitrescu CE. Improved thermodynamic model for lean natural gas spark ignition in a diesel engine using a triple Wiebe function. J Energy Resour Technol 2020 Jun 1;142(6).
[19] Liu J, Dumitrescu CE. Investigation of multistage combustion inside a heavy-duty natural-gas spark-ignition engine using 3D CFD simulations and the wiebe-function combustion model. J Eng Gas Turbines Power 2020 Jan 1;142(10).
[20] Duan X, Liu Y, Liu J, Lai MC, Jansons M, Guo G, Zhang S, Tang Q. Experimental and numerical investigation of the effects of low-pressure, high-pressure and internal EGR configurations on the performance, combustion and emission characteristics in a hydrogen-enriched heavy-duty lean-burn natural gas SI engine. Energy Convers Manag 2019 Sep 1;195:1319–33.
[21] Chen H, He J, Zhong X. Engine combustion and emission fuelled with natural gas: a review. J Energy Inst 2019 Aug 1;92(4):1123–36.
[22] Ouchikh S, Lounici MS, Tarabet L, Loubar K, Tazerout M. Effect of natural gas enrichment with hydrogen on combustion characteristics of a dual fuel diesel engine. Int J Hydrog Energy 2019 May 21;44(26):13974–87.
[23] Lee CF, Pang Y, Wu H, Hernández JJ, Zhang S, Liu F. The optical investigation of hydrogen enrichment effects on combustion and soot emission characteristics of CNG/diesel dual-fuel engine. Fuel 2020 Nov 15;280:118639.
[24] Hairuddin AA, Yusaf T, Wandel AP. A review of hydrogen and natural gas addition in diesel HCCI engines. Renew Sustain Energy Rev 2014 Apr 1;32:739–61.
[25] Das S, Kanth S, Das B, Debbarma S. Experimental evaluation of hydrogen enrichment in a dual-fueled CRDI diesel engine. Int J Hydrogen Energy 2022 Feb 9;47(20):11039–51.
[26] Ismael MA, Aziz AR, Mohammed SE, Baharom MB, Raheem AT, Ayandotun WB, et al. Experimental study on combustion stability and performance of hydrogen-enriched compressed natural gas of a free-piston linear generator. Int J Hydrogen Energy 2021 Nov 16;46(79):39536–47.
[27] Park C, Lee S, Kim C, Choi Y. A comparative study of lean burn and exhaust gas recirculation in an HCNG-fueled heavy-duty engine. Int J Hydrogen Energy 2017 Oct 12;42(41):26094–101.
[28] Liu YF, Liu B, Zeng K, Huang Z, Zhou L, Sun L. Performance and emission characteristics of a hydrogen-enriched compressed-natural-gas direct-injection spark ignition engine diluted with exhaust gas recirculation. Proc Inst Mech Eng - Part D J Automob Eng 2012 Jan;226(1):123–32.
[29] Zhao L, Wang D. Combined effects of cooled EGR and air dilution on butanol–gasoline TGDI engine operation, efficiency, gaseous, and PM emissions. ACS Omega 2020 Mar 23;5(12):6556–65.
[30] Imran S, Korakianitis T, Shaukat R, Farooq M, Condoor S, Jayaram S. Experimentally tested performance and emissions advantages of using natural-gas and hydrogen fuel mixture with diesel and rapeseed methyl ester as pilot fuels. Appl Energy 2018 Nov 1;229:1260–8.
[31] Mehra RK, Duan H, Luo S, Rao A, Ma F. Experimental and artificial neural network (ANN) study of hydrogen enriched compressed natural gas (HCNG) engine under various ignition timings and excess air ratios. Appl Energy 2018 Oct 15;228:736–54.
[32] Aydın M, Uslu S, Çelik MB. Performance and emission prediction of a compression ignition engine fueled with biodiesel-diesel blends: a combined application of ANN and RSM based optimization. Fuel 2020 Jun 1;269:117472.
[33] Yaliwal VS, Banapurmath NR, Soudagar ME, Afzal A, Ahmadi P. Effect of manifold and port injection of hydrogen and exhaust gas recirculation (EGR) in dairy scum biodiesel-low energy content gas-fueled CI engine operated on dual fuel mode. Int J Hydrog Energy 2022 Feb 1;47(10):6873–97.
[34] Uslu S. Optimization of diesel engine operating parameters fueled with palm oil-diesel blend: comparative evaluation between response surface methodology (RSM) and artificial neural network (ANN). Fuel 2020 Sep 15;276:117990.
[35] Hora TS, Agarwal AK. Effect of varying compression ratio on combustion, performance, and emissions of a hydrogen enriched compressed natural gas fuelled engine. J Nat Gas Sci Eng 2016 Apr 1;31:819–28.
[36] Verhelst S, Wallner T. Hydrogen-fueled internal combustion engines. Prog Energy Combust Sci 2009 Dec 1;35(6):490–527.
[37] Mabadi Rahimi H, Jazayeri SA, Ebrahimi M. Multi-objective optimization of a RCCI engine fueled with diesel fuel and natural gas enriched with hydrogen. Gas Processing Journal 2021 Jul 1;9(2):33–42.
[38] Balamurugan G, Gowthaman S. A review on split injection performances in DI diesel engine with different injection strategies and varying EGR using biodiesel as fuel. Mater Today Proc 2021 Feb 20.
[39] Balijepalli R, Kumar A, Rajak U, Elkotb MA, Alwetaishi M, Dasore A, Verma TN, Saleel CA, Afzal A. Numerical investigation of the effect of spray angle on emission characteristics of a diesel engine fueled with natural gas and diesel. Energy Rep 2021 Nov 1;7:7273–87.
[40] Bose PK, Maji D. An experimental investigation on engine performance and emissions of a single cylinder diesel engine using hydrogen as inducted fuel and diesel as injected fuel with exhaust gas recirculation. Int J Hydrog Energy 2009 Jun 1;34(11):4847–54.
[41] CFD A. Solver users guide [z]. AVL FIRE; 2013.
[42] Kostić O, Stefanović Z, Kostić I. CFD modeling of supersonic airflow generated by 2D nozzle with and without an obstacle at the exit section. FME Transactions 2015;43(2):107–13.
[43] de Morais AM, Justino MA, Valente OS, de Morais Hanriot S, Sodré JR. Hydrogen impacts on performance and CO2 emissions from a diesel power generator. Int J Hydrog Energy 2013 May 30;38(16):6857–64.
[44] Agarwal D, Singh SK, Agarwal AK. Effect of Exhaust Gas Recirculation (EGR) on performance, emissions, deposits and

durability of a constant speed compression ignition engine. Appl Energy 2011 Aug 1;88(8):2900–7.
[45] Williams CK, Rasmussen CE. Gaussian processes for machine learning. Cambridge, MA: MIT press; 2006.
[46] Arthur CK, Temeng VA, Ziggah YY. A Self-adaptive differential evolutionary extreme learning machine (SaDE-ELM): a novel approach to blast-induced ground vibration prediction. SN Appl Sci 2020 Nov;2(11):1–23.
[47] Snelson E, Ghahramani Z. Local and global sparse Gaussian process approximations. InArtificial Intelligence and Statistics 2007 Mar 11:524–31. PMLR.
[48] Arthur CK, Temeng VA, Ziggah YY. Soft computing-based technique as a predictive tool to estimate blast-induced ground vibration. J Sustain Mining 2019 Nov 1;18(4):287–96.
[49] Nocedal J, Wright SJ. Large-scale unconstrained optimization. Numerical Opt 2006:164–92.
[50] Anil R, Pereyra G, Passos A, Ormandi R, Dahl GE, Hinton GE. Large scale distributed neural network training through online distillation. arXiv preprint arXiv:1804.03235 2018 Apr 9.
[51] Li W, Liu Z, Wang Z, Dou H. Experimental and theoretical analysis of effects of atomic, diatomic and polyatomic inert gases in air and EGR on mixture properties, combustion, thermal efficiency and NOx emissions of a pilot-ignited NG engine. Energy Convers Manag 2015 Nov 15;105:1082–95.
[52] Hu E, Huang Z. Optimization on ignition timing and EGR ratio of a spark-ignition engine fuelled with natural gas-hydrogen blends. SAE Technical Paper; 2011 Apr 12.
[53] Zhou J, Guo Y, Huang Z, Wang C. A review and prospects of gas mixture containing hydrogen as vehicle fuel in China. Int J Hydrog Energy 2019 Nov 12;44(56):29776–84.
[54] Khodamrezaee F, Keshavarz A. Thermodynamic and experimental analysis of hydrogen addition to CNG in a spark ignition engine for emission reduction. Energy Sources, Part A Recovery, Util Environ Eff 2020 Apr 4:1–2.
[55] Park BY, Lee KH, Park J. Conceptual approach on feasible hydrogen contents for retrofit of CNG to HCNG under heavy-duty spark ignition engine at low-to-middle speed ranges. Energies 2020 Jan;13(15):3861.
[56] Hao D, Mehra RK, Luo S, Nie Z, Ren X, Fanhua M. Experimental study of hydrogen enriched compressed natural gas (HCNG) engine and application of support vector machine (SVM) on prediction of engine performance at specific condition. Int J Hydrog Energy 2020 Feb 14;45(8):5309–25.
[57] Huang Z, Huang J, Luo J, Hu D, Yin Z. Performance enhancement and emission reduction of a diesel engine fueled with different biodiesel-diesel blending fuel based on the multi-parameter optimization theory. Fuel 2022 Apr 15;314:122753.
[58] Kumar BR, Saravanan S, Rana D, Anish V, Nagendran A. Effect of a sustainable biofuel–n-octanol–on the combustion, performance and emissions of a DI diesel engine under naturally aspirated and exhaust gas recirculation (EGR) modes. Energy Convers Manag 2016 Jun 15;118:275–86.
[59] Kanth S, Ananad T, Debbarma S, Das B. Effect of fuel opening injection pressure and injection timing of hydrogen enriched rice bran biodiesel fuelled in CI engine. Int J Hydrog Energy 2021 Aug 13;46(56):28789–800.
[60] Zareei J, Rohani A, Mazari F, Mikkhailova MV. Numerical investigation of the effect of two-step injection (direct and port injection) of hydrogen blending and natural gas on engine performance and exhaust gas emissions. Energy 2021 Sep 15;231:120957.
[61] Lee S, Kim G, Bae C. Lean combustion of stratified hydrogen in a constant volume chamber. Fuel 2021 Oct 1;301:121045.
[62] Long Y, Li G, Zhang Z, Liang J. Application of reformed exhaust gas recirculation on marine LNG engines for NOx emission control. Fuel 2021 May 1;291:120114.